ELSEVIER

Chemical Engineering Science 62 (2007) 4112–4125

Chemical Engineering Science

www.elsevier.com/locate/ces

A new framework for solution of multidimensional population balance equations

Jayanta Chakraborty, Sanjeev Kumar*

Department of Chemical Engineering, Indian Institute of Science, Bangalore 560 012, India

Received 3 February 2007; received in revised form 13 April 2007; accepted 28 April 2007
Available online 17 May 2007

Abstract

A new framework is proposed in this work to solve multidimensional population balance equations (PBEs) using the method of discretization. A continuous PBE is considered as a statement of evolution of one evolving property of particles and conservation of their n internal attributes. Discretization must therefore preserve $n+1$ properties of particles. Continuously distributed population is represented on discrete fixed pivots as in the fixed pivot technique of Kumar and Ramkrishna [1996a. On the solution of population balance equation by discretization—I. A fixed pivot technique. Chemical Engineering Science 51(8), 1311–1332] for 1-d PBEs, but instead of the earlier extensions of this technique proposed in the literature which preserve 2^n properties of non-pivot particles, the new framework requires $n+1$ properties to be preserved. This opens up the use of triangular and tetrahedral elements to solve 2-d and 3-d PBEs, instead of the rectangles and cuboids that are suggested in the literature. Capabilities of computational fluid dynamics and other packages available for generating complex meshes can also be harnessed. The numerical results obtained indeed show the effectiveness of the new framework. It also brings out the hitherto unknown role of directionality of the grid in controlling the accuracy of the numerical solution of multidimensional PBEs. The numerical results obtained show that the quality of the numerical solution can be improved significantly just by altering the directionality of the grid, which does not require any increase in the number of points, or any refinement of the grid, or even redistribution of pivots in space. Directionality of a grid can be altered simply by regrouping of pivots.

Keywords: Multivariate population balance equations; PBE; PBM; Discretization

1. Introduction

Detailed modeling of a variety of particulate systems involving drops, bubbles, particles, biological cells, etc. requires information on population of particulate entities with different internal attributes, for example, population of drops and bubbles of different sizes and biological cells of different age. Hulburt and Katz (1964) and Randolph (1964) were the first to propose the framework of population balances in chemical engineering literature to model particulate processes. The range of particulate processes that can be modeled using the above framework is very large and is known since then. The use of population balance models (PBM), however, has seen a phenomenal growth only in the last 15 years or so. Among the many factors that have contributed to this growth, availability of simple and efficient discretization methods to solve population balance equations (PBEs) (Hounslow et al., 1988; Kumar and Ramkrishna, 1996a, 1997) is an important one. Effectiveness of these methods, developed for monovariate (1-d) PBEs, is quite clear from their widespread use.

In recent times, multidimensional PBM have became one of the principal areas of interest. In many fields of industrial importance, for example, granulation process or nanoparticle synthesis, 1-d model is inadequate. Iveson (2002) has pointed out that 4-d population balance is needed to model wet granulation process successfully. In a recent review, Cameron et al. (2005) suggest that significant economic gains are possible if granulation processes can be modeled accurately.

The use of PBM now appears to be limited by the availability of effective methods to solve multidimensional PBEs. In the present work, we propose a new framework to solve

* Corresponding author. Tel.: +91 80 2293 3110; fax: +91 80 2360 8121.
E-mail address: sanjeev@chemeng.iisc.ernet.in (S. Kumar).

0009-2509/$ - see front matter © 2007 Elsevier Ltd. All rights reserved.
doi:10.1016/j.ces.2007.04.049

multidimensional PBEs by using discretization methods. We believe that the new framework constitutes an *internally consistent* and natural extension of our 1-d fixed pivot technique (Kumar and Ramkrishna, 1996a,b) to higher dimensions.

The rest of the paper is organized as follows. We first present a brief review of the discretization methods for 1-d PBEs, followed by a review of the methods available to solve multidimensional PBEs. We then present the new framework for solving n-d PBEs, followed by the discretization equations and their ability to capture evolution of multivariate populations. Directionality of the grid and its manipulation to obtain improved solution, a hitherto unknown aspect and applicable only for the solution of 2-d and higher dimensional PBEs, is brought out and discussed at the end.

2. Previous work

2.1. Discretization methods for the solution of 1-d PBEs

A variety of numerical methods, such as orthogonal collocation, method of weighted residuals, collocation on finite elements, problem-specific polynomials, and finite difference, have been used over the years to solve PBEs (Ramkrishna, 1985, 2000) of the type given below:

$$\frac{\partial n(v,t)}{\partial t} = \frac{1}{2}\int_0^v n(v-v',t)n(v',t)Q(v-v',v')\,\mathrm{d}v' - \int_0^\infty n(v,t)n(v',t)Q(v,v')\,\mathrm{d}v'. \quad (1)$$

These methods were followed by the discretization method of the type proposed by Bleck (1970) and Seinfeld et al. (Gelbard and Seinfeld , 1978; Gelbard et al., 1980), in which population over a discrete size range is taken to be uniform and autonomy of the resulting equations is restored by using mean field approximation on number density. The final set of equations obtained has a number of double integrals in it which rapidly increase in number with an increase in the number of discrete ranges taken.

Hounslow et al. (1988) developed a new discretization technique which did not involve evaluation of any double integrals, conserved mass, and ensured correct evolution of total number of particles for geometrically increasing discretization range ($v_i = 2v_{i-1}$). This work came as a major breakthrough as all the techniques available till that time, excluding that of Sastry and Gaschignard (1981), could either conserve mass or correctly account for changes in number of particles. Hounslow et al. (1988) assumed stepwise uniform number density distribution and identified relevant events that change the size distribution. While deriving the discretized equations, they accounted for numbers correctly, but no measure was taken to conserve volume (mass). Mass conservation was accomplished by incorporating a correction factor and its value was estimated by forcing mass conservation. This factor turned out to be independent of the kernel. Kostoglou and Karabelas (1994), who carried out a comparative study of the discretization techniques available at that time, found the technique of Hounslow et al. (1988) to be the best. Litster et al. (1995) later extended the technique of Hounslow et al. (1988) to the grids of type $v_i = 2^{1/q}v_{i-1}$ where q is an integer.

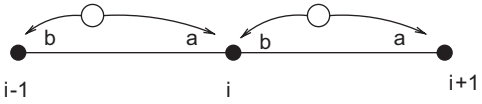

Fig. 1. Assignment of non-pivot particles of volume v to the neighboring pivots x_{i-1} and x_i in the fixed pivot technique of Kumar and Ramkrishna (1996a).

Kumar and Ramkrishna (1996a) presented a new discretization technique, which has come to be popularly known as *fixed pivot* technique in the literature. Fixed pivots are the pre-chosen discrete sizes which represent the continuously distributed population of particles. Thus,

$$n(v,t) \equiv \sum_i N_i(t)\delta(v-v_i). \quad (2)$$

Equations are written for the variation of population of particles of these discrete sizes. The central theme of the above technique is the new concept of *internal consistency* of discretization. The discretized set of equations for a PBE can be manipulated algebraically to obtain equations for the desired moments (or properties in general) of the size distribution. Internal consistency of discretization requires the equations obtained above to be identical to those obtained by discretization of the equations for the desired moments (or properties) directly, not just in the limit of a very fine grid but for an arbitrarily coarse grid as well. The internal consistency was achieved by representing events leading to the formation of non-pivot particles in a way so as to preserve the properties of the particles which correspond to the desired moments of the size distribution. Thus, if total mass (first moment) and the total number (zeroth moment) of the particles are the desired moments of the size distribution, internal consistency is maintained if non-pivot particles formed due to aggregation are assigned to the adjoining pivots while preserving number and mass. If fractions a and b are assigned to the pivots on the right and the left of the non-pivot particle as shown in Fig. 1, then

$$a+b=1, \quad ax_i + bx_{i-1} = v. \quad (3)$$

The above concept can be used to deal with non-pivot particles arising out of aggregation, breakup, growth, and nucleation. Furthermore, pivots can be distributed sparsely in some region and densely in some other region to improve the accuracy of the numerical solution.

Their discretized equation for the pure coalescence process is

$$\frac{\mathrm{d}N_i}{\mathrm{d}t} = \sum_{j,k}^{j\geqslant k}\left(1-\frac{1}{2}\delta_{j,k}\right)\eta Q_{j,k}N_jN_k - N_i\sum_{k=1}^{M}Q_{i,k}N_k, \quad (4)$$

where η is

$\eta = a$ for $(x_{i-1} \leqslant v \geqslant x_i)$,

$\eta = b$ for $(x_i \leqslant v \geqslant x_{i+1})$.

Vanni (2000) has carried out a detailed comparison of the above technique with the other techniques for their robustness, and the accuracy of solution they produce under a variety of situations. Based on the simplicity of implementation and the accuracy of the solution produced, he suggests fixed pivot method as the method of choice for the general case of aggregation–fragmentation problems. Attarakih et al. (2004) who have extended the above technique for spatially distributed drop population in extraction columns have also provided a critique of the various other techniques. They find the fixed pivot technique to be quite robust for using it as the starting point for the development of numerical techniques for simulation of systems involving additional phenomena.

The fixed pivot scheme when combined with coarse distribution of pivots tends to over-predict size distribution in the size range in which number density decreases steeply with particle volume (tail region). Often, the fraction of population contained in this size range is quite small and is not a cause of concern. Nonetheless, if required, this situation can be remedied easily with the use of densely distributed pivots in the tail region, an option not available with the earlier techniques in this class.

Kumar and Ramkrishna (1996a) have analyzed the above problem of over-prediction for a coarse grid. They find that the cause of over-prediction is the placement of a pivot in the middle of a notional bin while the location of the average of the particle size for a bin may be towards the left boundary for sharply decreasing number density and towards the right boundary for sharply increasing number density. Kumar and Ramkrishna (1996b) proposed a new moving pivot technique to address this problem. The position of the pivot in this technique moves from near the left boundary for sharply decreasing number density towards the center as the number density over this size range evolves with time and becomes less steep. The location of the pivot is determined by preserving two desired properties of the size distribution. For example, if mass and number are the desired properties, the equation for the location of the pivot in ith cell for pure aggregation is given by

$$\frac{\mathrm{d}x_i}{\mathrm{d}t} = \frac{1}{N_i}\sum_{j,k}^{j\geqslant k}\left(1-\frac{1}{2}\delta_{j,k}\right)[(x_j+x_k)-x_i]Q_{j,k}N_jN_k.$$

This equation is coupled with the discretized PBE (similar to Eq. (4)) for number density to get a closed system. Kumar et al. (2006) have recently combined the above idea of the moving pivot with the fixed pivot technique to develop a new technique which retains the simplicity of fixed pivot technique and achieves the accuracy of moving pivot technique.

2.2. Solution of multidimensional PBEs

The generalized version of Eq. (1) for multidimensional population undergoing aggregation is given by

$$\frac{\partial n(\mathbf{v},t)}{\partial t} = \frac{1}{2}\int\int Q(\mathbf{v}',\mathbf{v}'')n(\mathbf{v}',t)n(\mathbf{v}'',t)P(\mathbf{v}'+\mathbf{v}''|\mathbf{v})\,\mathrm{d}\mathbf{v}'\mathrm{d}\mathbf{v}'' - \int_0^\infty Q(\mathbf{v}',\mathbf{v})n(\mathbf{v},t)n(\mathbf{v}',t)\,\mathrm{d}\mathbf{v}', \quad (5)$$

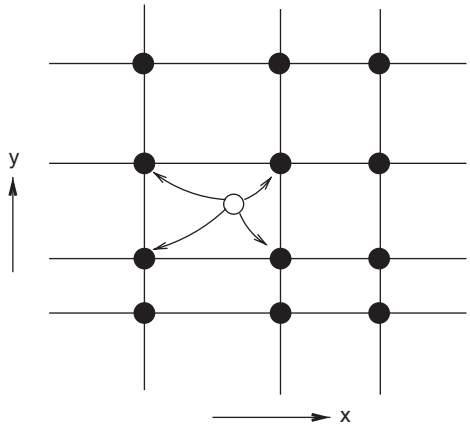

Fig. 2. Rectangular array of pivots in 2-d space, used in straightforward extension of fixed pivot technique of Kumar and Ramkrishna (1996a).

where $\mathbf{v}$ is a vector of internal coordinates that identifies a particle uniquely. For liquid–liquid extraction, $\mathbf{v}$ consists of drop volume, concentration of various solutes in it, and its age if penetration theory of mass transfer is to be used. In the case of crystallization, $\mathbf{v}$ consists of particle volume and crystal habit, and, in the case of reverse micelles used for nanoparticle synthesis, $\mathbf{v}$ consists of concentrations of reactants and products, and the size of nanoparticle, if any.

Early efforts to solve multidimensional PBE have focused on reduction of internal coordinate with some suitable assumptions. Pilinis (1990) used the assumption that all the particles of a given size have identical composition to reduce the dimensionality of the problem. Although this assumption produced satisfactory results, no theoretical basis is available. Obrigkeit et al. (2004) approximated composition for every particle size by a finite series of orthogonal basis function. Immanuel and Doyle (2005) employed a hierarchical two-tier technique in order to solve 3-d PBE containing aggregation and consolidation terms.

2.3. Discretization methods for multidimensional PBEs

Given the widespread use of discretization methods to solve PBEs, efforts have been made to extend these methods to multidimensional PBEs as well. Kumar and Ramkrishna (1995) were the first to extend their fixed pivot technique to solve bivariate population balances which arise in liquid–liquid extraction operations. In this straightforward extension, the pivots were generated on a rectangular grid, as shown in Fig. 2, to approximate the 2-d number density as

$$n(x,y,t) \equiv \sum_i\sum_j N_{i,j}\delta(x-x_i,y-y_j). \quad (6)$$

A non-pivot particle is first split along one of the internal directions using the preservation of the desired properties as in 1-d fixed pivot technique, and then along the other internal direction. Thus, to represent a particle of volume x containing solute amount y, it is first split along x direction as 'a' particle with attribute (x_i, y) and 'b' particle with attribute

(x_{i+1}, y). These two populations, yet not located on pivots, are then split along the y direction to represent them as 'r' particles of attribute (x_i, y_j), 's' particles of attribute (x_i, y_{j+1}), 't' particles of attribute (x_{i+1}, y_j), and 'u' particles of attribute (x_{i+1}, y_{j+1}). One non-pivot particle is thus represented through four surrounding pivots. For preservation of numbers and conservation of volume x and solute y in this manner, we thus have

$$a + b = 1, \quad ax_i + bx_{i+1} = x,$$
$$r + s = a, \quad ry_j + sy_{j+1} = ay,$$
$$t + u = b, \quad ty_j + uy_{j+1} = by. \tag{7}$$

Vale and McKenna (2005) have also extended the 1-d fixed pivot technique to 2-d aggregation for rectangular grid of pivots (Fig. 2). They proposed a non-pivot particle to be represented through four surrounding pivots in such a way that its four properties—number, two internal coordinates x and y, and their product xy—are preserved exactly. If the fractions assigned to neighboring pivots (x_i, y_j), (x_i, y_{j+1}), (x_{i+1}, y_j), (x_{i+1}, y_{j+1}) are r, s, t, and u, respectively, then

$$r + s + t + u = 1,$$
$$rx_i + sx_i + tx_{i+1} + ux_{i+1} = x,$$
$$ry_j + sy_{j+1} + ty_j + uy_{j+1} = y,$$
$$rx_iy_j + sx_iy_{j+1} + tx_{i+1}y_j + ux_{i+1}y_{j+1} = xy. \tag{8}$$

The above four simultaneous equations can be solved simultaneously to obtain fractions r, s, t, and u. It can be shown that $ru = st$, and, hence, the systems of equations (7) and (8) are identical. Two techniques are thus identical, with the final set of discretized equation for aggregation of bivariate population being given as

$$\frac{dN_{i,j}}{dt} = \sum_{k,l}\sum_{r,s}\left(1 - \frac{1}{2}\delta_{k,r}\delta_{l,s}\right)\eta_{i,j}^{k,l,r,s}\beta_{kl,rs}N_{kl}N_{rs} - N_{ij}\sum_{k,l}\beta_{ij,kl}N_{kl}.$$

Representation of a non-pivot particle thus requires four surrounding pivots for a 2-d PBE, eight for a 3-d PBE, 16 for a 4-d PBE, and 2^n for an n-d PBE.

We propose a new framework in the next section to discretize multidimensional PBEs. It requires a non-pivot particle for an n-d PBE to be represented by $n + 1$ surrounding neighbors, instead of 2^n pivots. This framework is not only an *internally consistent* extension of our 1-d fixed pivot technique (Kumar and Ramkrishna, 1996a) but also a more powerful one for solving multidimensional PBEs.

3. Formulation of discrete equations

A monovariate PBE, for example, Eq. (1) for aggregation of particles, is a statement of evolution of one evolving property and conservation of one internal property of particles. The evolving property can be a *number* of particles which evolve from two to one after one aggregation event, and the conserved quantity can be particle *volume* which remains unchanged after the event. Only two distinct properties of the aggregated particle need to be specified correctly to track the evolving size distribution. These can be number and mass of particle, or other properties such as surface area and perimeter which also permit unique identification of spherical particles. In the case of a bivariate PBE, three and only three *distinct* properties need to be specified to identify particles uniquely. In the simplest case, for example, in liquid–liquid extraction, these can be *volume*, *amount* of solute in particles, and *number* of particles. In general, new particles with n internal attributes require only $n + 1$ distinct particle properties to be specified for their identification. These can be n internal attributes of particles and their number. It needs to be stressed that identification of n internal attributes alone does not identify particles uniquely, as formation of particle volume x_1 and solute amounts $x_2, x_3, \ldots$ can be represented through either *one* particle of volume x_1 containing solute amounts $x_2, x_3, \ldots$ in it *or* n particles of volume x_1/n containing solute amounts $x_2/n, x_3/n, \ldots$ in them, or anyone of the many other combinations that are also possible.

In view of the above, a minimum of $n + 1$ properties need to be preserved to represent non-pivot particles with n internal attributes. The fixed and the moving pivot techniques proposed for the solution of 1-d PBEs already implement it. Extension of the 1-d *moving pivot technique* to solve bivariate PBEs requires a pivot located in 2-d plane to have two degrees of freedom along the two axes representing internal coordinates to respond to the evolving shape of the bivariate number density over the bin. The moving pivot technique thus requires two equations for the movement of the pivot and one equation for particle population for each bin, irrespective of the shape of the bin. The above three equations follow from the preservation of three properties of particles—numbers, and the two internal attributes x and y which are conserved. Similar arguments applied to the solution of an n-d PBE using the moving pivot technique require preservation of $n + 1$ properties to yield n equations for the movement of a pivot in n-d space and one equation of the population of particles in bin. Thus, the generalized moving pivot technique is consistent with the minimum number of properties that need to be preserved for an internally consistent discretization technique. In fact, the moving pivot technique can preserve only the minimum number of attributes.

Extension of the 1-d fixed pivot technique to bivariate PBEs has so far been carried with the four properties instead of the minimum three required. If the same strategy is followed to extend the fixed pivot technique to higher dimensional PBEs, preservation of eight properties instead of the minimum four is required for 3-d PBEs, preservation of 16 properties instead of the minimum five is required for 4-d PBEs, and so on. This is because the discretization is tied to the rectangular shape of the bin used in these extensions. Thus, if the 2-d space of bivariate PBEs is discretized with space filling pentagons, five properties of non-pivot particles would have to be preserved to represent

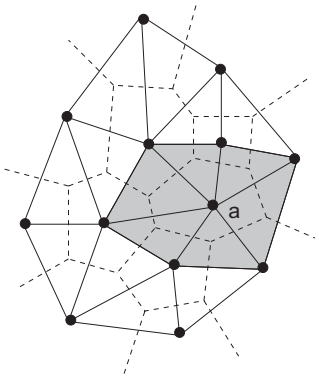

Fig. 3. Division of 2-d space using natural elements, and the arbitrary distribution of pivots made possible for the new framework proposed in this work.

it through the five surrounding pivots located on the vertices of the pentagons.

We propose to preserve the minimum number of properties required for an internally consistent discretization of n-d PBEs for the fixed pivot technique, and choose the shape of the bin accordingly. Solution of an n-d PBE requires a bin with $n+1$ vertices in n-d space. Thus, we propose to use triangular shape bins in 2-d space for bivariate PBEs, tetrahedrons in 3-d space for trivariate PBEs, and a shape with $n+1$ vertices in n-d hyperspace.

3.1. Subdivision of space—triangulation

It is interesting to note that the idea of using bins with minimum number of $n+1$ vertices in n-d space is already a well-known one in computational geometry. Given that the particle population is represented on pivots, if the pivots are distributed arbitrarily in 2-d plane, they cannot be connected to form regular rectangular bins. An alternative in this case is to use Voronoi partitioning (Aurenhammer, 1991), as shown in Fig. 3. If two points in a Voronoi construction share a common Voronoi side, they are called natural neighbors. By connecting natural neighbors (pivots), we get a triangulation known as Delaunay triangulation, and the shapes that we get are known as *natural elements*. This process leads to triangles as natural elements for 2-d spaces, tetrahedrons as natural elements for 3-d spaces, and so on. Natural elements with $n+1$ vertices offer the minimum possible points required in n-d space to define a shape that encloses an n-d region. Hence, when it comes to represent a non-pivot particle through pivots, natural elements disperse the non-pivot particle populations to the minimum possible number of pivot populations—$n+1$ pivots for natural elements vs. 2^n pivots for hypercuboid elements.

The partitioning of space using natural elements is unique in nature. It is, however, not essential, and the proposed framework works equally well with other kinds of triangulation. The Voronoi cells in n-d space are analogous to subspace between v_i and v_{i+1} in 1-d space, and the (Delaunay) triangles are analogous to the subspace between two pivots, from x_i to x_{i+1}. While the division of 2-d and 3-d spaces into rectangles and cuboids is easy to handle, we will see shortly that the use of triangles and tetrahedrons opens new possibilities for increasing accuracy and efficiency of the proposed framework through (i) reduced dispersion, because reduced number of pivots are required to represent non-pivot particles, and (ii) flexible distribution of pivots, dense in some local region or along an arbitrary curve and sparse elsewhere in n-d space.

The discretization strategy used in the fixed pivot technique for 1-d PBE holds for the solution of multidimensional PBEs as well. The first step in discretization is the generation of pivots on which particle population is represented. We permit the pivots to be distributed on an irregular grid so that they can be adapted to any situation. It is best to identify individual pivots in such a collection by tagging them with an integer index. Thus, we propose to use the following approximation for number density:

$$n(\mathbf{v},t)=\sum_{k=1}^{M}N_k(t)\delta(\mathbf{v}-\mathbf{x_k}), \tag{9}$$

where $\mathbf{v}$ and $\mathbf{x_k}$ are n-d vectors. $\mathbf{x_k}$'s represent locations of the pivots. In contrast to Eq. (6), which requires pivots to be located on a regular rectangular grid, Eq. (9) permits pivots to be distributed in space without any restrictions. It also reduces to Eq. (2) simply by converting vectors $\mathbf{v}$ and $\mathbf{x_k}$ to scalars for 1-d space.

Such a general and flexible distribution of pivots requires us to 'triangulate' them, which refers to grouping of $(n+1)$ pivots together (in n-d space) to construct elements and indexing of these elements. Many standard algorithms for triangulation are available in the standard texts (Preparata and Shamos, 1985). One can make use of commercial CFD softwares Fluent and CFX, mathematical softwares MATLAB and MATHEMATICA, and open source software GTS to carry out triangulation and indexing of the triangulated elements. In this work, we have used Fluent for this purpose.

Triangulated elements thus represent domains with $n+1$ pivots as vertices. Any non-pivot particle that falls in this domain as a result of the particulate processes is represented through particle population of the surrounding $n+1$ pivots. A determination of the element to which a newly formed particle belongs is an important step. This determination is made for the 1-d case very simply by satisfying inequalities such as $x_{i-1}<(x_j+x_k)<x_{i+1}$. In higher dimensional space, such a search is not trivial as one needs to know which triangle or tetrahedron out of a large number of those present contains a given point $(\mathbf{x_j}+\mathbf{x_k})$ *inside* it. This search, however, needs to be carried only once at the time of generation of pivots.

There are different search algorithms available in the literature to accomplish the above task. The algorithm of Kirkpatrick (1983) is optimum and quite efficient (number of steps required) in marching towards the element that contains the point of interest, but it is somewhat complex to implement. We have instead implemented a simpler search routine called directional search, explained in detail by Devillers et al. (2002).

3.2. Derivation of discretized equations

Integrating Eq. (5) over a Voronoi-type region in n-d space, we have

$$\frac{dN_i(t)}{dt} = \frac{1}{2}\int_{\odot i} d\mathbf{v} \int_{\mathbf{0}}^{\mathbf{v}} Q(\mathbf{v}', \mathbf{v}-\mathbf{v}')n(\mathbf{v}', t)n(\mathbf{v}-\mathbf{v}', t)\, d\mathbf{v}' - \int_{\odot i} d\mathbf{v} \int_{\mathbf{0}}^{\infty} Q(\mathbf{v}', \mathbf{v})n(\mathbf{v}, t)n(\mathbf{v}', t)\, d\mathbf{v}', \quad (10)$$

where the $\odot i$ represents ith sub-domain, and $N_i(t)$ is the total number of particles in it at time t. A single index denotes subdivisions for multidimensional space. This will generate discretized equations identical to those for 1-d case, with the dimensionality of the problem being buried in the indices assigned to the elements. It is easy to revert back to dimensional representation by referring to the hash of element index and element location in space.

To preserve $n+1$ properties, we generalize the strategy used in 1-d fixed pivot technique (Kumar and Ramkrishna, 1996a) for n dimensions. We split each particle ($\mathbf{v}=\mathbf{x_j}+\mathbf{x_k}$) generated at a non-grid location (non-pivot point), and assign these fractions to populations at pivots which form vertices of the natural element in which the non-pivot particle is located. The fraction assigned to each pivot is solely determined by preserving $n+1$ properties. Let us represent $n+1$ fractions by $f_i(\mathbf{v}, \mathbf{x_i})$, $i=1, 2, \ldots, (n+1)$. The equations which preserved properties $P_j(\mathbf{v})$, $j=1, 2, \ldots, (n+1)$, are given by

$$\sum_i f_i(\mathbf{v}, \mathbf{x_i}) \times P_j(\mathbf{x_i}) = P_j(\mathbf{v}), \quad j=1, 2, \ldots, (n+1)$$

which can be solved simultaneously to obtain fractions f_i.

The above process for assignment of non-pivot particles combined with the fixed pivot technique yields the following equation for aggregation of particles in multidimensional problems. We have not provided many steps involved in derivation here as these closely follow the procedure already provided in detail by Kumar and Ramkrishna (1996a). Interested reader is referred to it for details.

$$\frac{dN_i}{dt} = -N_i(t)\sum_j Q_{i,j}N_j(t) + \sum_{j,k}^{j\geqslant k}\left(1-\frac{1}{2}\delta_{j,k}\right)\eta^i_{j,k}Q_{j,k}N_jN_k. \quad (11)$$

Here, $\eta^i_{j,k} = f_i(x_j + x_k, x_i)$ is called coefficient matrix. It represents the fraction of particle assigned to population at ith pivot when particles represented by jth and kth pivots aggregate and preserve P_j properties of the aggregated particle, where $j=1, 2, \ldots, (n+1)$. Clearly, matrix $\eta^i_{j,k}$ forms the core of the entire technique. Its structure does not change with the dimensionality of the problem. Since the elements of this matrix do not change with the form of the aggregation kernel or the evolving population of the particles, in principle, it can be generated along with the grid and stored forever for use.

4. Results and discussion

Very few analytical solutions are available for multidimensional PBEs. A general solution for aggregation of particles with n internal coordinates is available for constant kernel (Gelbard et al., 1980) with the following general initial condition:

$$n_0(x_1, x_2, \ldots, x_m) = N_0\prod_{i=1}^{m}\frac{(p_i+1)^{(p_i+1)}x_i^{p_i}}{\Gamma(p_i+1)x_{i0}^{p_i+1}} \times \exp\left[-(p_i+1)\frac{x_i}{x_{i0}}\right]. \quad (12)$$

The above initial size distribution reduces to exponential distribution for $p_i=0$ and gamma distribution for $p_i=1$. x_{i0} indicates the value of average mass for ith internal variable, and is taken to be 0.08 for all internal variables in all the simulations reported here, unless stated otherwise. The exact analytical solution for the case described above is (Gelbard et al., 1980)

$$n(x_1, x_2, \ldots, x_m, t) = \frac{4N_0}{(\tau+2)^2}\prod_{i=1}^{m}\frac{(p_i+1)^{(p_i+1)}}{x_{i0}} \times \exp\left[\frac{-(p_i+1)x_i}{x_{i0}}\right] \times \sum_{k=0}^{\infty}\left(\frac{\tau}{\tau+2}\right)^k \times \prod_{j=1}^{m}\frac{[(p_j+1)^{(p_j+1)}]^k(x_j/x_{j0})^{(k+1)(p_j+1)-1}}{\Gamma[(p_j+1)(k+1)]}. \quad (13)$$

Sum kernel was also studied in this work. Its form is taken to be $Q(\mathbf{v}, \mathbf{v}') = x + x'$, which indicates that the aggregation frequency depends only on the mass of one internal variable x. This is physically justified as coalescence of drops depends only on their volumes if the solute dissolved in drops is not surface active.

Three kinds of grids have been used in the present work to obtain numerical solutions. The first one consists of the rectangular/cuboid-type grid which is generated first by populating the axes with geometrically spaced pivots and then meshing the domain by using straight lines parallel to the axes and passing through these pivots. This grid requires preservation of 2^n properties. The second kind of grid is generated by converting the above grid elements to those with only $n+1$ vertices. Thus, the rectangles were divided into triangles by introducing diagonal lines and the cuboids were converted into tetrahedrons by cutting it with planes (shown later). It is important to note that these modifications of the grid do not change the number and position of pivots in space, and therefore the number of discretized equations that need to be solved remains unchanged.

The third type of grid is generated by using Fluent. As Fluent is geared to generate computational grid for real geometries, it can produce well-meshed grids comprising of triangular elements in 2-d and tetrahedral elements in 3-d space on linear scale. Since the internal variables of PBEs range over several decades, we have stretched the linear grid generated by Fluent using a function of our choice, but without altering the

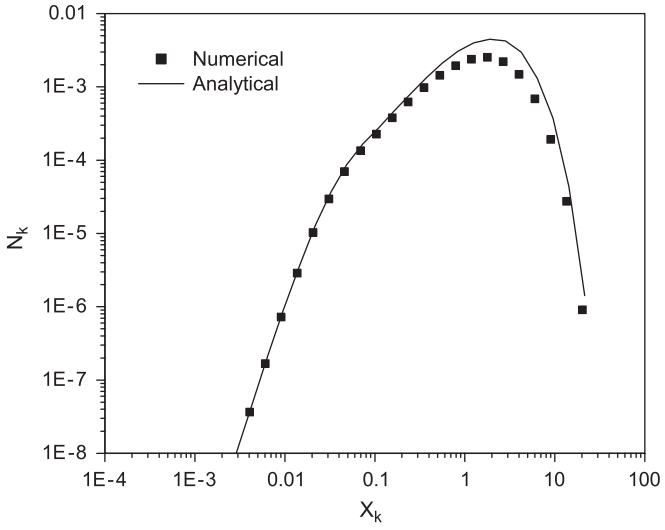

Fig. 4. Comparison of numerical and analytical solutions for particle population on pivots located on the diagonal for a regular rectangular grid consisting of 676 pivots. The particle population is initially gamma distributed, and the extent of evolution corresponds to $N(t)/N(0) = 0.047$. $x_k = y_k$ for diagonal pivots.

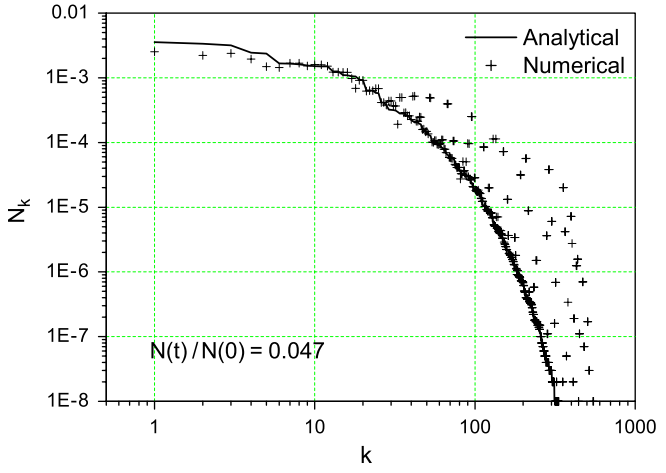

Fig. 5. Flat representation of numerical and analytical solution for particle population at all the pivots. The other details are the same as those for Fig. 4.

connectivity between the grid points, thus obviating the need for retriangulation of grid points. The capabilities available in various packages mentioned above can therefore be harnessed to generate grids which comprise triangles/tetrahedrons, and are refined along an arbitrarily chosen direction or in a region, as desired for the problem at hand.

The system of coupled first order differential equations (Eq.(11)) was solved by adaptive step Runge–Kutta method, taken from Press et al. (2002).

Effectiveness of the various numerical techniques to solve PBEs is demonstrated through a comparison of the numerically obtained populations at pivots with those obtained analytically. The latter are obtained by integrating the analytical solution given by Eq. (13) over the enclosure of a particular pivot (shown by the shaded area in Fig. 3 for pivot located at point 'a'). Integration was carried out by using Monte Carlo method. Each randomly selected point in the region of interest provides a population to the pivot located at the vertices of the region. This process is the same as that followed to assign a non-pivot particle at that location to the pivots surrounding it.

The code written to test the ideas developed in this work was first tested for its ability to reproduce results reported in the literature with minimum alterations in the code. We have reproduced the results of Vale and McKenna (2005), contained in their Fig. 4, for constant kernel and for the same extent of evolution ($N(t)/N(0) = 0.0196$), using the same rectangular grid as theirs (40×40, with a geometric ratio of 1.5 for both the axes) for the preservation of four properties of non-pivot particles, viz. number (x^0y^0), mass (x^1y^0), mass (x^0y^1), and product of masses (x^1y^1). The results are identical, hence they are not shown here to save space.

Fig. 4 shows results for the same kernel for smaller number of grid points (26×26) and for reduced extent of evolution of $N(t)/N(0) = 0.047$ for initially gamma distributed population. The figure shows particle populations on pivots located on the diagonal, obtained analytically and numerically using rectangular grid for the preservation of four properties mentioned above. The figure clearly shows that the numerical results obtained are in good agreement with the analytical results. Fig. 4 of Vale and McKenna (2005) also compares their numerical predictions with analytical results for pivots located only on the diagonal.

Such a comparison leaves out populations on a large number of pivots, located off-diagonally. It is possible to devise other methods such as 3-d plots for 2-d PBEs to show a comparison of the numerical and the analytical results. Some of these methods lead to very cluttered plots for higher dimensional problems while the others can be used only for 2-d PBEs. In view of the above, we have adopted in this work a simple method to compare the numerical and the analytical results. As the discretized equations lose the dimensionality of the problem because the bins are identified by an index assigned to them, we compare the results by plotting analytically and numerically obtained particle populations at pivots vs. a new index assigned to pivots by sorting analytically obtained populations at pivots in decreasing order. Thus, the pivot with the smallest index has the highest population and the larger indices carry diminishing populations. Such a plot on logarithmic scales resolves pivots of higher population very well and covers the entire size domain. We have named it as *flat representation* as one can examine the quality of solution by looking at one single plot. The other details such as the regions of over- and under-prediction are hidden, however. This method also comes to rescue when the diagonal of the domain does not necessarily pass through the pivots.

Fig. 5 provides a comparison of populations at all the pivots for the case discussed above (Fig. 4). Figs. 4 and 5 show that while the particle populations on pivots along the diagonal are predicted quite well, the populations at other pivots are not in good agreement.

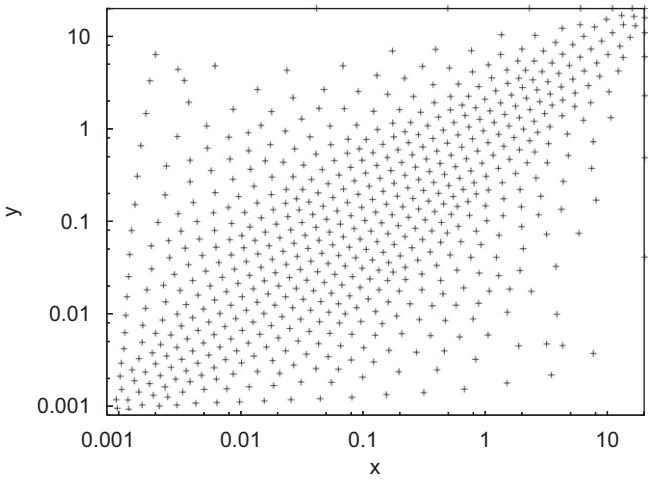

Fig. 6. The Fluent generated 2-d grid with selective refinement along the diagonal for a total of 653 grid points.

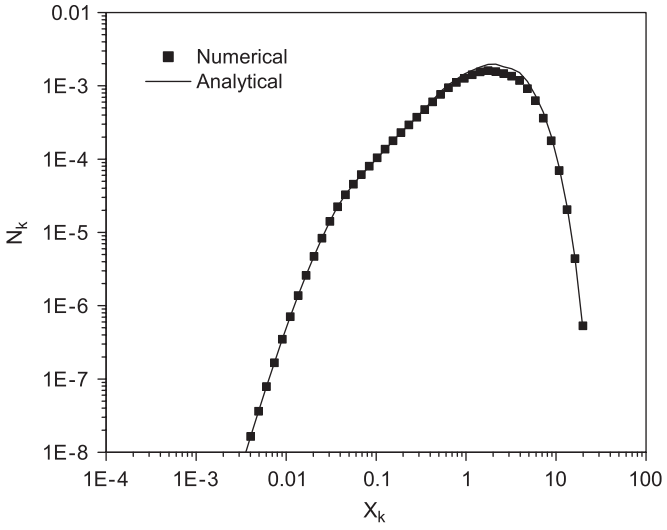

Fig. 7. Same as that for Fig. 4 for the grid shown in Fig. 6.

We have next solved the same 2-d problem using the preservation of three properties—number, and masses x and y, the minimum required for an internally consistent discretization using a triangular grid, shown in Fig. 6. The figure shows that the grid spans several decades of range for both the internal variables. As explained earlier in this section, this grid was generated using Fluent which can generate selectively refined grid in linear space. In this case, the diagonal was first populated with densely distributed grid points (pivots). A 2-d mesh was generated from these starting points in both the directions perpendicular to the diagonal. The grid was progressively coarsened in regions farther away from diagonal. This grid was then stretched using functions $x^{\text{new}} = c_1 \exp(c_2 x^{\text{old}})$ and $y^{\text{new}} = c_1 \exp(c_2 y^{\text{old}})$ to convert it to uniform grid on logarithmic scale.

In the present case, grids on the two sides of the diagonal are approximate mirror images of each other but this is not required. For asymmetric kernels (with respect to internal variables), one can make use of the power inherent in commercial packages to weave a denser mesh in any region of the computational domain, not just along the diagonal.

Fig. 7 shows a comparison of the numerical and analytical results for the pivots located along the diagonal for the same case as that considered in Figs. 4 and 5. The quality of this solution, obtained by using 653 pivots and preservation of three properties, numbers, and two masses, is better than that presented in Fig. 4 for the preservation of four properties on rectangular-type grid with 676 pivots. The x and y ranges covered by both the grids are nearly identical, and they both result in negligible mass loss from the upper end.

Fig. 8 shows a comparison of the evolution of first few moments of the size distribution with their analytical counterparts. The dimensionless time is defined as $t = N_0\beta_0 \times$ real time. In general, moment $M^{(ij)}$ based on continuous number density is defined as

$$M^{(ij)}(t) = \int_0^\infty \mathrm{d}x \int_0^\infty \mathrm{d}y x^i y^j n(x, y, t).$$

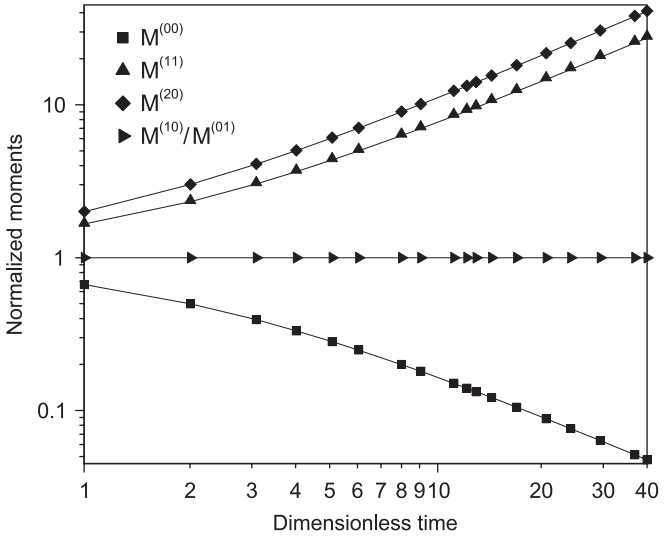

Fig. 8. A comparison of analytical and numerical solutions for time variation of moments of the size distribution for Fluent generated grid shown in Fig. 6. The other details are the same as those for Fig. 7.

In terms of discrete population (Eq. (9)), the same is obtained as

$$M^{(ij)}(t) = \sum_{k=1}^{M} x_k^i y_k^j N_k(t).$$

In the discretization scheme, properties x^0y^0, x^1y^0, x^0y^1 of non-pivot particles were preserved. Since x^1y^0 and x^0y^1 are also conserved before and after a particulate event, moments $M^{(10)}$ and $M^{(01)}$ are expected to remain unchanged with time. The figure indeed confirms it. The total number of particles ($M^{(00)}$) decreases with time due to aggregation, and the present technique, like its 1-d counterpart, predicts this evolution perfectly. The figure shows that with the fine grid employed along the diagonal, moments $M^{(11)}$ and $M^{(20)}$ which correspond to

non-preserved properties x^1y^1 and x^2y^0 are also predicted quite well.

Fig. 9 compares the full size distribution with the analytical one using flat representation. This figure should be compared with the comparison provided in Fig. 5 for rectangular grid. Fig. 9 shows many more points than those present in Fig. 5. This is because the pivots with populations smaller than 1×10^{-8} do not show up in the plot, and the rectangular grid results in a large number of such pivots. The two figures show that refinement of grid along the diagonal results in significant improvement in under-prediction of the largest populations, represented on the extreme left side of the plots. As the largest particle populations often also contain significant amount of dispersed phase in them, the improvement brought about is substantial in absolute terms.

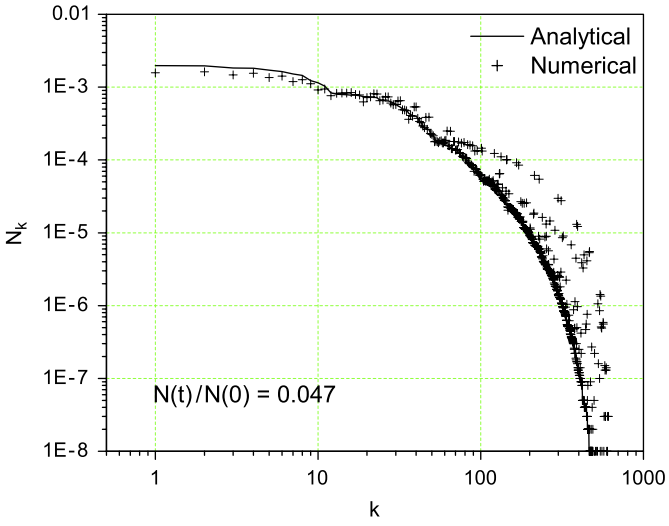

Fig. 9. Same as that for Fig. 5, but for the grid shown in Fig. 6.

The numerical results show over-prediction in the range of small populations in the form of clusters of points, each cluster appearing as a branch originating from the main curve. There are about five such clusters in Fig. 5, some of which correspond to quite large over-predictions. Preservation of three properties and the use of a flexible grid consisting of arbitrarily shaped triangles, refined along the diagonal and coarsened elsewhere, reduce the number of branches representing over-predicted populations to about three, for slightly smaller number of pivots. The overall agreement achieved thus is much improved with nearly the same number of pivots.

It is worthwhile to look at the nature of the solution for the 2-d case before we discuss results for the 3-d PBEs. Fig. 10 shows analytical solution for the above case. It shows that the number density decreases far more steeply on the two sides of the main diagonal than along the diagonal itself. Thus, unless special measures are taken to improve the solution in this zone, over-predictions are likely to be significant, as discussed by Kumar and Ramkrishna (1996a). A grid fine enough to capture the tail of the size distribution along the diagonal is perhaps not adequate for capturing very sharply decreasing number density in directions perpendicular to it. This is corroborated by the results presented in Figs. 5 and 9. Branches of points in these figures correspond to pivot populations in directions perpendicular to the diagonal. Although the Fluent generated grid is refined along the diagonal and also in the direction perpendicular to it, it is not fine enough to eliminate over-prediction in this region. It is encouraging to note that the flexibility provided by the new framework allows us to improve predictions significantly. The predictions can be further improved without increasing the number of pivots excessively, which would have not been possible with a rectangular grid.

Simulations similar to those presented above were also carried out for 3-d PBEs for constant kernel and gamma distribution as initial condition. Both, a rectangular grid consisting of

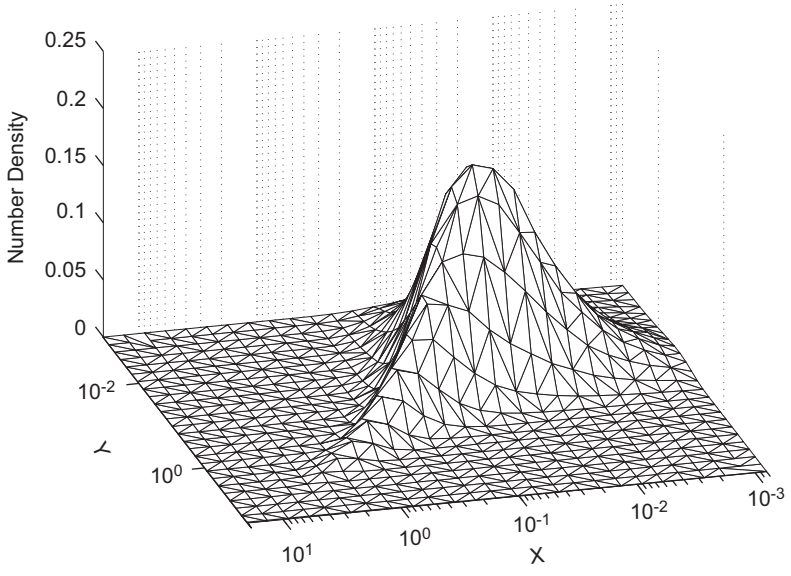

Fig. 10. The 3-d visualization of the analytically computed 2-d number density for constant kernel and initially gamma distributed population, for extent of evolution corresponding to $N(t)/N(0) = 0.047$.

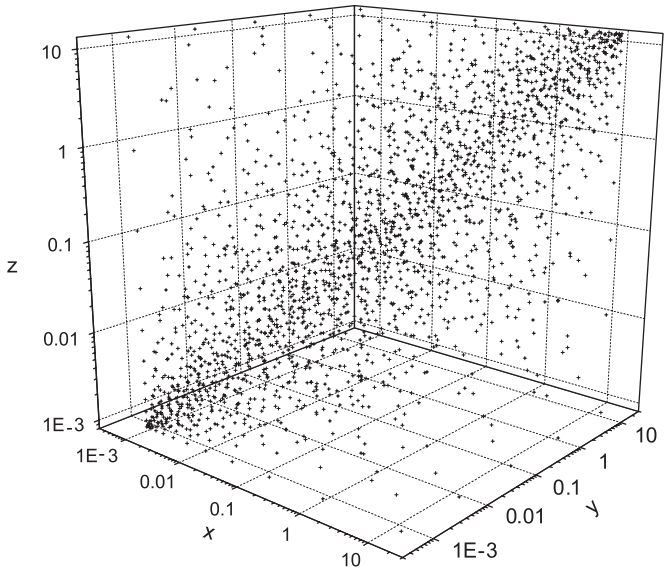

Fig. 11. The 3-d grid generated by Fluent for a total of 2195 pivots with refinement along the diagonal.

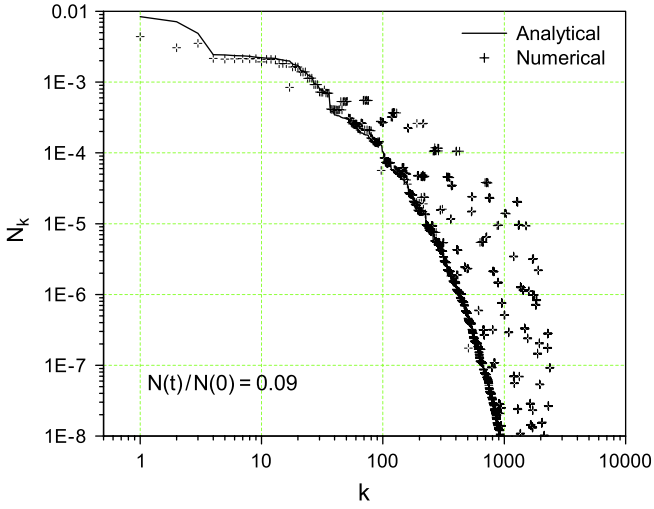

Fig. 12. Flat representation of numerical and analytical solution for 3-d PBE for initially gamma distributed particle population for constant kernel for an evolution of $N(t)/N(0) = 0.09$. The numerical solution is obtained using a cuboidal grid with preservation of eight properties on 3375 (15^3) pivots.

cuboid elements and a flexible grid consisting of tetrahedral elements were used to obtain numerical solution. The regular grid consists of 15 pivots in each of the three coordinate directions for the three internal coordinates (with a total of 3375 pivots), and requires eight properties to be preserved. In the present case, these were chosen to be $x^0y^0z^0$, $x^1y^0z^0$, $x^0y^1z^0$, $x^0y^0z^1$, $x^1y^1z^0$, $x^0y^1z^1$, $x^1y^0z^1$, $x^1y^1z^1$. A grid consisting of 2195 pivots was generated using Fluent, first in linear space and then stretched along the three directions to cover several decades of range for each internal coordinate. The final grid used is shown in Fig. 11. Only four properties of the non-pivot elements need to be preserved for this technique, $x^0y^0z^0$, $x^1y^0z^0$, $x^0y^1z^0$, and $x^0y^0z^1$.

Fig. 12 shows a comparison of numerically obtained populations at pivots with those obtained analytically for an evolution of $N(t)/N(0) = 0.09$ for cuboidal grid. The same results, obtained using the tetrahedral grid shown earlier (Fig. 11), are presented in Fig. 13. As seen before, cuboidal grid results in significant under-prediction of the largest populations in the system in absolute terms and significant over-prediction of smaller populations in relative terms. Use of tetrahedral elements with refinement in desired direction allows the solution to be improved significantly even while the number of pivots used is reduced from 3375 to 2195. Tetrahedral grid can be further refined to improve the quality of solution without increasing the number of pivots substantially. If the same degree of improvement is desired with a cuboidal grid, it would require a huge increase in the number of pivots as the grid would have to be refined in the entire computational domain. Once again, the meshing capabilities of CFD packages can be harnessed to solve multidimensional PBEs effectively. Unfortunately, this capability of CFD packages stops at 3-d domains, and special efforts are required to develop adaptive grids in higher dimensions.

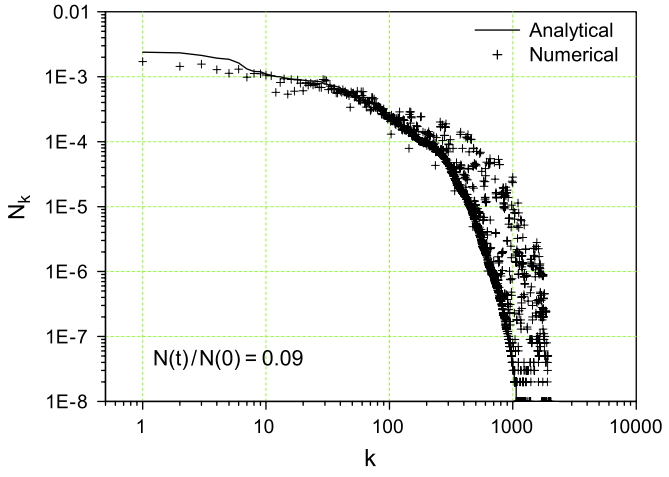

Fig. 13. Same as that for Fig. 12. Numerical results are obtained using Fluent generated grid shown in Fig. 11.

Simulations have also been carried out for sum kernel of form $Q(\mathbf{v}, \mathbf{v}') = x + x'$, where $\mathbf{v} = \{x, y, z\}$. The grid used to obtain numerical solution for this kernel is the same as that used to obtain the results shown in Fig. 13. Since an analytical solution for number density for this kernel is not available, we have computed moments for the numerically obtained size distribution and compared those with analytically obtained moments. The results are presented in Fig. 14. An accurate prediction of the complete size distribution requires a fine grid along the diagonal for constant kernel itself. A sum kernel is expected to show still poorer agreement between the two, and yet Fig. 14 shows that moments of the size distribution are predicted quite well. This holds very well for those moments for which the associated properties are preserved in discretization scheme, such as $M^{(000)}$, $M^{(100)}$, $M^{(010)}$, and $M^{(001)}$. As the properties associated with the last three moments are both

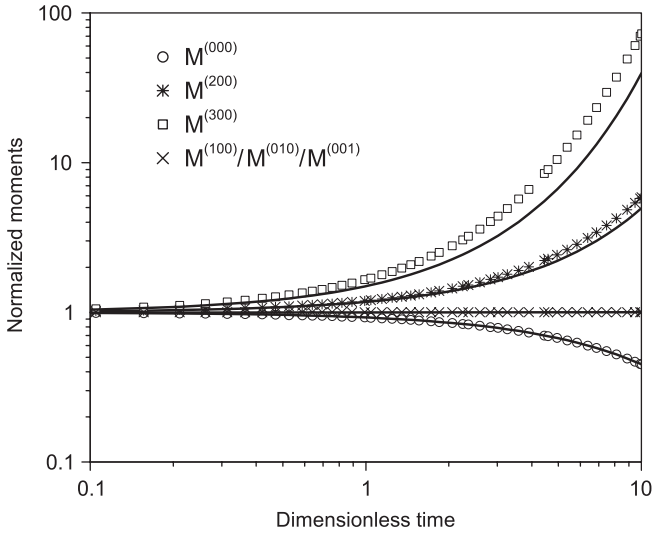

Fig. 14. A comparison of analytical and numerical solutions for time variation of moments for 3-d PBE. The numerical results are obtained by using the grid shown in Fig. 11 for sum kernel for an evolution of $N(t)/N(0) = 0.09$.

preserved and conserved, they remain unchanged with time. The variation of moments $M^{(200)}$ and $M^{(300)}$, which correspond to non-preserved properties, is not predicted well. A similar situation arises with the solution of 1-d PBE. Kumar and Ramkrishna (1996a) have shown that a fine grid in the regions of steeply decreasing number density improves the agreement significantly.

5. Directionality of grid

One of the simplest ways to implement the idea of bin elements with $n+1$ vertices for preservation of $n+1$ properties is to convert the rectangular elements used in earlier works into smaller elements with desired number of vertices without creating any new pivots. This also provides strict evaluation of the benefit that one can derive from the proposed framework.

A rectangular grid in 2-d space can be converted to have only triangular elements in it in two ways, as shown in Fig. 15. Let us call the arrangement on the left side as *along* triangles (whose diagonal is aligned with the diagonal of the 2-d space) and that on the right-hand side as *across* (whose diagonal is across the diagonal of the 2-d space).

Figs. 16 and 17 show predictions for aligned and across configuration of the elements, respectively. These results should also be compared with those shown in Fig. 5 for rectangular grid for identical location of the pivots. A comparison of the numerical results for the three methods of discretization for identical distribution of pivots shows that the aligned triangles produce the best agreement between the numerical and the analytical results, which is much better than the rest two. This is followed by the agreement obtained for rectangular grid. Triangular elements of across configuration produce results with the poorest agreement with the analytical results.

To understand the cause for this behavior, let us consider a 2-d population consisting of particles located on the diagonal,

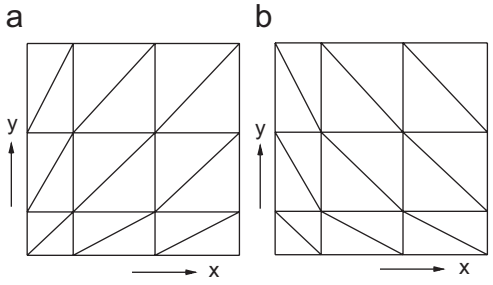

Fig. 15. *Along* (a) and *across* (b) arrangement of triangles.

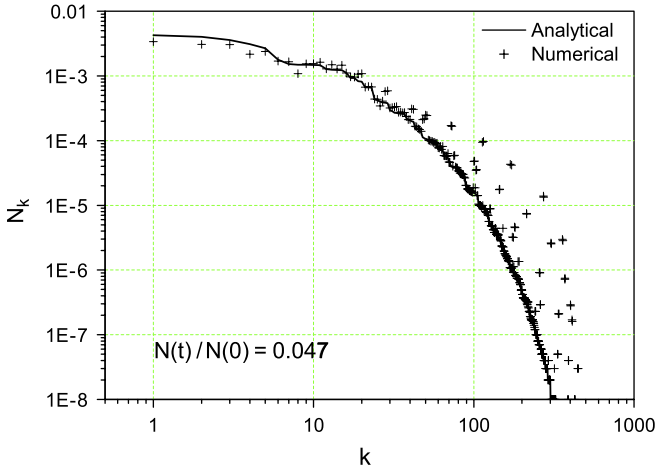

Fig. 16. Same as that for Fig. 5, but with orientation of triangles *along* the diagonal.

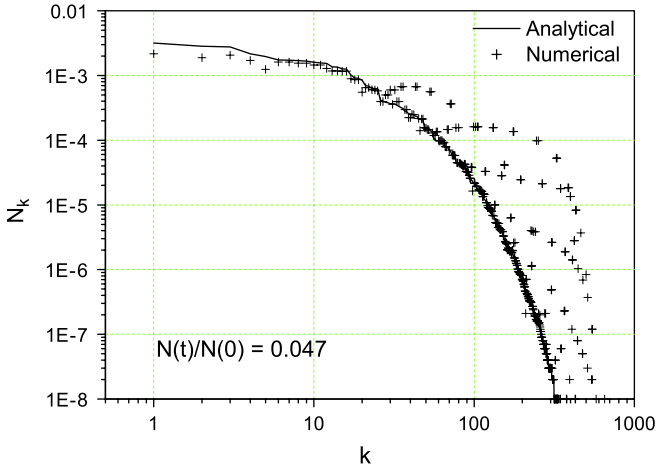

Fig. 17. Same as that for Fig. 5, but with orientation of triangles *across* the diagonal.

as shown in Fig. 18. In real terms, it only means that all the particles considered have the same ratio of two internal variables x and y in them. When such a population of particles evolves due to aggregation (coalescence) of particles, the new particles formed have the same ratio of internal variables and must remain located on the diagonal at all times. A rectangular grid which requires preservation of four properties does not ensure

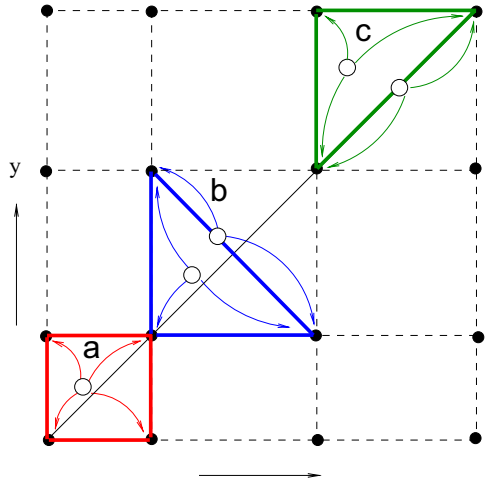

Fig. 18. Dispersion of a non-pivot entity with various element shapes: uniform dispersion with rectangular element (a), enhanced *across* dispersion (b) with *across* triangles, and enhanced *along* dispersion with *along* (c) triangles.

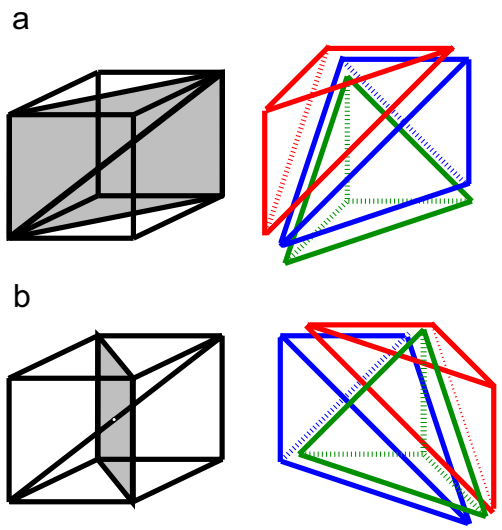

Fig. 19. Partitioning of a cuboid into six tetrahedrons with elements oriented *along* (a) and *across* (b) the diagonal.

it. A non-pivot particle is spread among four points in space, two of which are not on the diagonal. This is shown by the non-zero fractions assigned to these pivots. Thus, in this representation, particles with nearly same ratio of internal variables lead to the formation of many more particles with different ratios of internal variables than happens actually. The numerical solution thus gets dispersed in direction perpendicular to the diagonal. The use of initially gamma distributed population in two variables produces a similar situation, and therefore causes significant over-prediction in directions perpendicular to the diagonal.

With triangular elements in along configuration, shown in Fig. 18, and preservation of only three properties, particles formed on the diagonal are represented through pivots located on the diagonal itself. There is dispersion of particle population in the direction of the diagonal (as seen with 1-d fixed pivot technique), but there is no dispersion of these particles in directions perpendicular to the diagonal as the fraction allotted to the pivots on the third vertex is identically zero if internal attributes of particles are preserved in their representation. This has indeed been ensured in all the results presented in this work. The present framework thus permits a more accurate solution to be obtained without any refinement of the grid or redistribution of the pivots, simply by reducing the numerical dispersion. The above arguments are further corroborated by the results obtained for across triangles. Fig. 17 shows that the agreement is poorer than that obtained for the rectangular grid. In rectangular grid, a non-pivot point located on the diagonal is mostly assigned to the pivots on the diagonal and only small fractions are assigned to the pivots located away from the diagonal, so as to preserve the fourth property *xy* of the particles. In the case of the across arrangement of triangles, most of the particle formed on the diagonal is represented through pivots located off-diagonally, even when property *xy* of the particle is not preserved. Clearly, over-prediction in directions perpendicular to the diagonal must be the largest for the across arrangement of triangles.

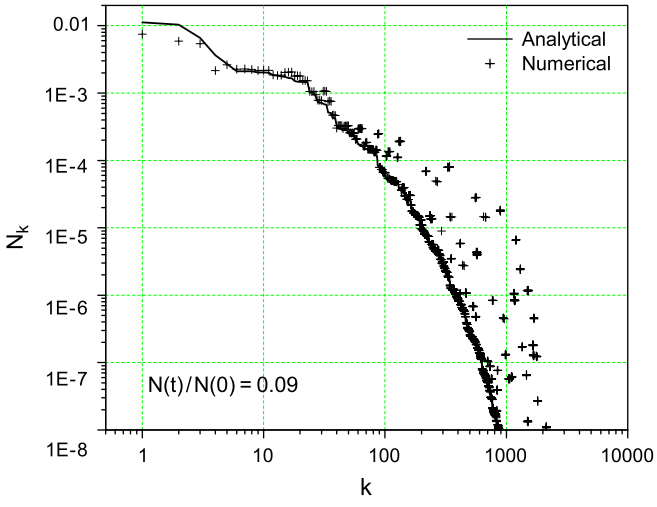

Fig. 20. Same as that for Fig. 12, but with tetrahedrons oriented *along* the diagonal.

The use of a flexible grid, which was refined along and near the diagonal using Fluent, improved the numerical solution as seen earlier (Fig. 9). The improvement could have been substantial, however, if the triangular grid could have been refined as well as aligned in the desired direction. Presently, it is not possible to control the orientation of the triangles using commercial packages. We have, however, developed a method which allows control on both of these aspects of a grid. This will be communicated later.

A similar exercise has been carried out for 3-d discretization as well. Here, rectangular grid generates cuboids requiring eight properties to be preserved. These cuboids can be converted to tetrahedrons, which require preservation of minimum four properties for internally consistent discretization, in at least two ways, as shown in Fig. 19.

Figs. 20 and 21 show a comparison of the numerical and the analytical solution for tetrahedron in along and across

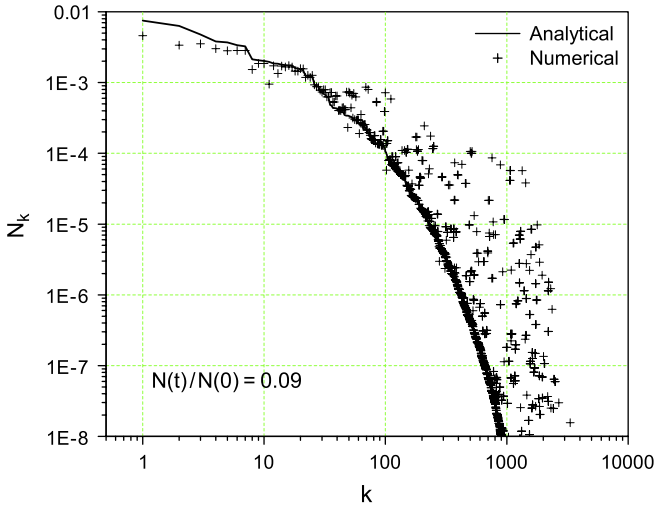

Fig. 21. Same as that for Fig. 12, but with tetrahedrons oriented *across* the diagonal.

orientations, respectively. Please notice that the number of pivots and the distribution of pivots in the 3-d space are identical for all the cases considered here. These results should also be compared with those presented in Fig. 12 for cuboids. As noted earlier for 2-d, the aligned tetrahedrons produce best agreement with the analytical solution. This is followed by the results obtained using regular cuboids. The poorest agreement is obtained for across configuration of tetrahedrons.

We thus find that in addition to the refinement of grid elements, directionality or orientation of the elements used for discretization, hitherto unknown, also plays an important role in controlling the accuracy of the numerical solution of multidimensional PBEs.

6. Conclusions

A new framework is proposed in this work which generalizes our 1-d fixed pivot technique (Kumar and Ramkrishna, 1996a) to solve n-d PBEs. According to this framework, a minimum of $n+1$ properties need to be preserved to obtain an internally consistent discretization of n-d PBEs. Earlier extension of the fixed pivot technique to solve n-d PBEs requires preservation of 2^n properties. The new framework thus invokes the use of triangular elements for numerical solution of 2-d PBEs and tetrahedral elements for 3-d PBEs. These are also the natural elements which can enclose a volume domain in n-d space with minimum number of vertices. The new framework facilitates refinement of computational grid in a local domain or along an arbitrary curve in n-d space without any restrictions. Grids with local refinement along the diagonal direction, generated using 2-d and 3-d meshing capabilities of Fluent, indeed show that quite accurate numerical solutions of multidimensional PBEs are possible with relatively small number of pivots concentrated along the direction of evolution of the solution. The proposed framework thus opens possibilities for harnessing capabilities of mesh generation packages to solve PBEs effectively.

A new issue brought out by the proposed framework is the significant role of directionality of a grid in controlling the quality of numerical solution of multidimensional PBEs. It is shown here that sub-optimal orientation of elements in n-d space can disperse the numerical solution quite substantially just as the preservation of more than the minimum number of properties does. The best strategy for solving multidimensional PBEs must therefore involve the use of minimal internally consistent discretization schemes, with the grid elements refined and properly directed in the region of significant population so as to contain numerical dispersion. More work is required to address the issue of orientation of grid elements and their shapes to arrive at robust techniques for solving multidimensional PBEs accurately and efficiently.

References

Attarakih, M.M., Bart, H.-J., Faqir, N.M., 2004. Numerical solution of the spatially distributed population balance equation describing the hydrodynamics of liquid liquid dispersions. Chemical Engineering Science 59, 2567–2592.

Aurenhammer, F., 1991. Voronoi diagram—a survey of a fundamental geometric data structure. ACM Computing Survey 23 (3), 345–405.

Bleck, R., 1970. A fast, approximate method for integrating the stochastic coalescence equation. Journal of Geophysical Research 75, 5165–5171.

Cameron, I.T., Wang, F.Y., Immanuel, C.D., Stepanek, F., 2005. Process systems modelling and applications in granulation: a review. Chemical Engineering Science 60, 3723–3750.

Devillers, O., Pion, S., Teillaud, M., 2002. Walking in a triangulation. International Journal of Foundations of Computer Science 13, 181–199.

Gelbard, F.M., Seinfeld, J.H., 1978. Coagulation and growth of a multicomponent aerosol. Journal of Colloid and Interface Science 63 (3), 472–479.

Gelbard, F.M., Tambour, Y., seinfield, J.H., 1980. Sectional representations for simulating aerosol dynamics. Journal of Colloid and Interface Science 76, 541–556.

Hounslow, M.J., Ryall, R.L., Marshall, V.R., 1988. A discretized population balance for nucleation, growth, and aggregation. A.I.Ch.E. Journal 34 (11), 1821–1832.

Hulburt, H.M., Katz, S., 1964. Some problems in particle technology. Chemical Engineering Science 19, 555–574.

Immanuel, C.D., Doyle, F.J., 2005. Solution technique for a multi-dimensional population balance model describing granular processes. Powder Technology 156, 213–225.

Iveson, S.M., 2002. Limitations of one dimensional population balance models of wet granulation processes. Powder Technology 124, 219–229.

Kirkpatrick, D., 1983. Optimal search in planar subdivision. SIAM Journal on Computing 12 (1), 28–35.

Kostoglou, M., Karabelas, A.J., 1994. Evaluation of zero order methods for simulating particle coagulation. Journal of Colloid and Interface Science 163, 420–431.

Kumar, J., Peglow, M., Warnecke, G., Heinrich, S., Morl, L., 2006. Improved accuracy and convergence of discretized population balance for aggregation: the cell average technique. Chemical Engineering Science 61, 3327–3342.

Kumar, S., Ramkrishna, D., 1995. A general discretization technique for solving population balance equations involving bivariate distributions. In: A.I.Ch.E. Annual Meeting, Miami Beach, FL, USA, November 12–17. Paper No. 139c.

Kumar, S., Ramkrishna, D., 1996a. On the solution of population balance equation by discretization—I. A fixed pivot technique. Chemical Engineering Science 51 (8), 1311–1332.

Kumar, S., Ramkrishna, D., 1996b. On the solution of population balance equation by discretization—II. A moving pivot technique. Chemical Engineering Science 51 (8), 1333–1342.

Kumar, S., Ramkrishna, D., 1997. On the solution of population balance equations by discretization—III. Simultaneous nucleation, growth and aggregation. Chemical Engineering Science 52, 4659–4679.

Litster, J.D., Smit, D.J., Hounslow, M.J., 1995. Adjustable discretized population balance for growth and aggregation. A.I.Ch.E. Journal 41 (3), 591–603.

Obrigkeit, D.D., Resch, T.J., McRae, G.J., 2004. Integrated framework for the numerical solution of multicomponent population balances. 2. The split composition distribution method. Industrial and Engineering Chemistry Research 43, 4394–4404.

Pilinis, C., 1990. Derivation and numerical solution of the species mass distribution equations for multicomponent particulate system. Atmospheric Environment 24A (7), 1923–1928.

Preparata, F., Shamos, M.I., 1985. Computational Geometry: an Introduction. Springer, Berlin.

Press, W.H., Teukolsky, S.A., Vetterling, W.T., Flannery, B.P., 2002. Numerical Recipes in Fortran 90, second ed. Cambridge University Press, Cambridge.

Ramkrishna, D., 1985. The status of population balances. Reviews in Chemical Engineering 3, 49–95.

Ramkrishna, D., 2000. Population Balances: Theory and Applications to Particulate Systems in Engineering. Academic Press, San Diego.

Randolph, A.D., 1964. A population balance for countable entities. The Canadian Journal of Chemical Engineering 280–281.

Sastry, K.V.S., Gaschignard, P., 1981. Discretization procedure for the coalescence equation of particulate process. Industrial and Engineering Chemistry, Fundamentals 20, 355–361.

Vale, H.M., McKenna, T.F., 2005. Solution of the population balance equation for two-component aggregation by an extended fixed pivot technique. Industrial and Engineering Chemistry Research 44, 7885–7891.

Vanni, M., 2000. Approximate population balance equations for aggregation breakage processes. Journal of Colloid and Interface Science 221, 143–160.